Daagu International Journal of Basic and Applied Research 7(2) (2025): 751-773
doi: 10.20372/dijbar150.v7i2.2025

Research Article

Groundwater prospect zonation using the analytical hierarchy process technique in Mekelle area, Tigray, northern Ethiopia

Kahsay Hailekiros[*1], Tesfamichael Gebreyohannes[2] and Abdelwassie Hussein[2]

[1]Mekelle Industrial Park, Industrial Park Development Corporation (IPDC), Mekelle, Tigray, Ethiopia
[2]Department of Geology, School of Earth Science, Mekelle University, P.O.Box 3066, Mekelle, Tigray, Ethiopia
*Corresponding author email: hakiros2000@gmail.com

Received: December 6, 2024 *Revised: September 23, 2025* *Accepted: November 05, 2025*

Abstract

This study is aimed to delineate groundwater prospect zones of Mekelle area using Analytical Hierarchy process techniques. Eight thematic layers including geomorphology, geology, lineament density, slope, drainage density, soil, land use/cover and precipitation were used for the groundwater prospect zone mapping. The weighted sum overlay Analysis method in the ArcGIS environment was used to map the groundwater prospect zones of the study area. The results of the groundwater prospect zone were validated using yields of 42 deep wells, 29 shallow wells and 29 springs. Accordingly, the groundwater prospect of the area classified into four zones as poor, moderate, good and very good with respective area coverage of 185 km^2, 252 km^2, 243 km^2 and 358 km^2. The correlation of the geology and the prospect zones shows that areas covered with the deep massive dolerite aquifers represent poor groundwater prospect zones, while the shallow, weathered and fractured dolerite and shale-marl-limestone intercalations correspond to the moderate groundwater prospect zones. Whereas, the lower sandstone formation is correlated with good prospect zones as well as the marl-limestone and limestone-marl formations with intensive lineament concentrations are corresponded with the very good prospect zones. Validation of the groundwater prospect zones against the corresponding yield variations of the groundwater point's results in a fit of about 94%.

Keywords: Analytical Hierarchy Process, Weighted Sum Overlay Analysis, Groundwater Prospect Zones, Mekelle

1. INTRODUCTION

The conventional hydrogeological techniques of groundwater exploration using geophysical methods are expensive and time-consuming (Fetter, 1994; Sener et al., 2005; Nsiah et al., 2018). Hence identification

of the groundwater prospect zones demands latest technologies including GIS and remote sensing that can help investigate large areas in a short period of time with limited resources. These Remote sensing and GIS approaches have been applied to delineate groundwater prospect zones by a number of researchers throughout the world (Agarwal et al., 2013; Sar et al., 2015; Yeh et al., 2016; Pinto et al., 2017; Siva et al., 2017; Thapa et al., 2017; Al-Shabeeb et al., 2018; Gnanachandrasamy et al., 2018; Murmu et al., 2019; Singh et al., 2019). Groundwater prospect zone mapping using the weighted overlay analysis depend on geology, geomorphology (landforms), slope, soil type, rainfall, land use and drainage parameters (Thapa et al., 2017; Murasingh et al., 2018). The analytic hierarchy process (AHP) approach is one of the most extensively used multi-criteria decision-making models (Arulbalaji et al., 2019; Murmu et al., 2019). AHP is mainly considered as a simple, transparent, effective, and reliable system (Ishizaka and Labib, 2011), and hence can be used for delineating groundwater prospect zones (Patra et al., 2018). The APH technique was applied in Golina River Basin, Northern Ethiopia by (Gebru et al., 2020). In this study area, some regional scale PhD hydrogeological studies like Tesfamichael (2009) and Girmay (2015) as well as several local studies were conducted. Among these studies Abdelwassie (2000) investigated the hydrogeology of the Aynalem valley south of Mekelle. WWDSE (2007) made a comprehensive investigation of the Aynalem well field, which supplies drinking water for Mekelle. However, most of these studies use the conventional methods and none of these previous studies deal with delineation of groundwater prospect zones using Analytical Hierarchy Process. Hence, objective of this study is to develop the map of groundwater Prospect Zones for Mekelle area (30-kilometer radius of Mekelle City) using weighted sum overlay analysis of the thematic layers in ArcGIS environment.

2. MATERIALS AND METHODS

2.1. Study area description

Mekelle area is found in the northeastern part of the Ethiopian central plateau to the west of the Afar Depression. The study area is part of the Geba catchment and belongs to the Tekeze drainage system. This study area includes catchments within 30 km radius of Mekelle city, Capital of Tigray Regional state, and covers an area of about 1,038 km^2. Geographically, it is bounded by latitudes of 1465136 to 1512585m North and longitudes of 531219 to 578803m East UTM (Figure 1). The study area is accessible with the main asphalt road of Addis Ababa -Mekelle, Mekelle - Adigrat and Samre – Mekelle roads cross in the south to north direction while the Temben - Mekelle, Mekelle - Quiha - Aragure and the Mekelle - Quiha

- Abaala roads cross in the West to east direction (Figure 1). Small gravel roads which connect small villages and quarries branch from the main asphalt roads and play their role in improving accessibility.

The topography of the study area is highly controlled by erosional features and geological structures. The elevation of the area varies from 1,576 m a.m.s.l in the western part of the area to 2,762 m a.m.s.l in the eastern part. The area is characterized by deep gorges and cliffs of limestone and chain of dolerite ridges, which have been intruded as sills and dykes. The slope ranges 0° – 76°. It is drained by four main rivers namely the Chelekot/Gabat, Aynalem, Illala and May Mekden Rivers that flow towards the west and joining the Geba River in the western boundary. Most of the seasonal tributaries feed the main streams both from north and south which have substantial runoff during the rainy season. The drainage density in the study area is 0.60 km/km^2 and the streams have a dendritic drainage pattern.

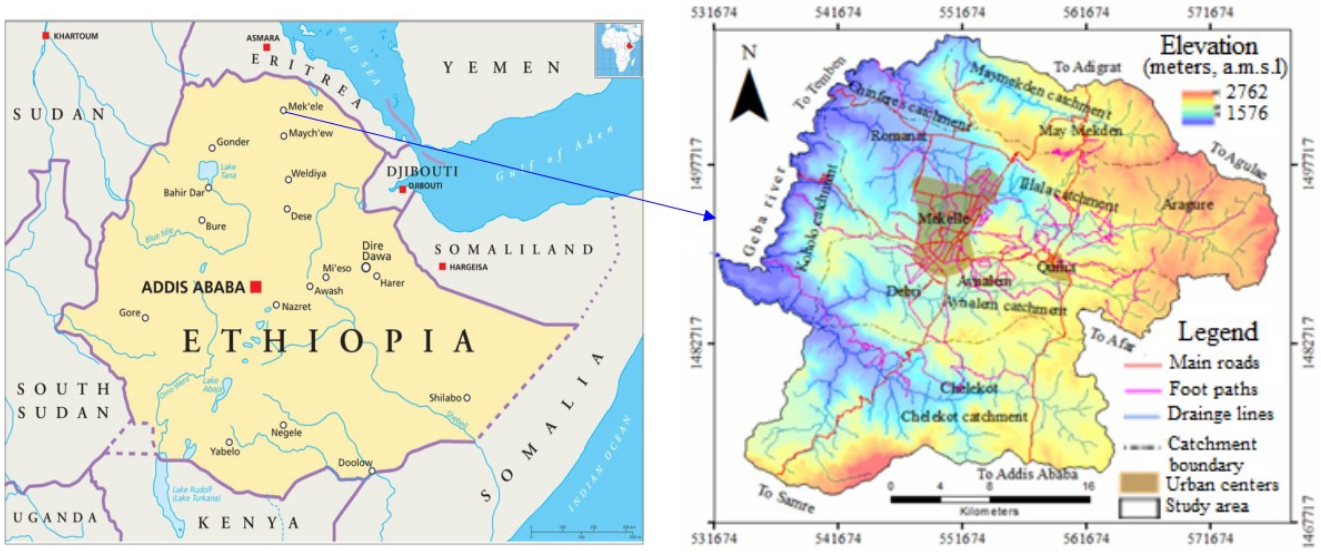


Figure 1. Location map of the study area. (a.m.s.l. stands for above mean sea level).

The region is characterized by a semi-arid climate, with a mean annual precipitation ranging from 391 to 646 mm year. The rainy season, known as `Kiremt`, is confined to a short period from June to September. The remaining eight months of the year are generally dry, with occasional light precipitation in some areas. The air temperature ranges from an average daily minimum of 13.97 ºC to an average daily maximum of 18.47 ºC. In general, the north Ethiopian rainfall regime is under the influence of both the Indian and the Atlantic Ocean monsoons (Daniel, 1977; Griffiths et al., 1972 Telford, 1998; Kebede and Travi, 2012). The flow of the monsoon moisture to the region is controlled by the seasonal migration of the Inter Tropical Convergence Zone (ITCZ). During the wet season (June to September), the ITCZ is

located in northern Ethiopia and is under the influence of the southwesterly and southerly monsoon flows while the ITCZ is located south of Ethiopia during the dry season (between October and March) which results in northerly flow of dry and cold air from the Arabian continent (Daniel, 1977; Kebede and Travi, 2012).

The Land-use/land cover of the study area is categorized in to seven classes which include: cultivated agricultural land with scattered trees, shrub land, bare land, grass land, water body, settlement of rural community and urban areas and forest. Four soil textural classes have been identified in the area which are: Sandy clay loam, Silty loam, Clay loam and Silty clay loam.

The geology includes the rock formations such as Lower Adigrat Sandstone, Antalo Limestone, Transitional Facies, Agulae Shale Formation, Amba-Aradam Formation, Tertiary Volcanics and Doleritic rocks, and Quaternary Deposits (Alluvial sediments and Carbonate precipitates) (Tesfamichael, 2009). The catchments are affected by the main fault belts named as Mekelle fault belt and Chelekot fault belt oriented nearly Northwest-Southeast direction and other sets of synthetic faults and lineaments trending NW-SE, NE-SW and N-S directions. The intensity of major and minor fractures varies from one lithology to another and this may be due to the geological properties of the various units. Strong fracturing is noted in the Antalo limestone whereas in the Mekelle dolerite, the intensity of fracturing is very low as compared to the other adjacent units. Most of the synthetic faults oriented in NW direction are observed around May Mekden and Chinferes catchments, almost perpendicular to the Mekelle fault belt, faults trending in the NE direction are found widely distributed throughout the Illala catchment and those oriented to the SE direction are noted on the upper Chelekot catchment.

2.2. Methodology

The groundwater prospect zones were identified using the weighted sum overlay analysis techniques in ArcGIS, using geology, lineament density, slope, drainage density, soil and land use land cover layers from the study area. Weights of these thematic layers and their classes were assigned using the concepts of Analytical Hierarchy Process (Arulbalaji et al., 2019). Finally, the groundwater prospect zones were validated using 42 deep wells, 29 shallow wells and 29 springs.

2.2.1. Preparation of thematic layers

The first major step in groundwater prospect zone mapping involved delineating both the study area boundary and the required thematic layers. In this study, the boundary was defined using a Digital Elevation Model (DEM) of northern Ethiopia. The DEM was obtained from the Advanced Land

Observing Satellite (ALOS) Phased Array L-band Synthetic Aperture Radar (PALSAR) with a 12.5 m spatial resolution (DAAC, 2015).

Groundwater prospect zones were mapped using eight thematic layers: geomorphology, geology, lineament density, slope, drainage density, soil, land use/land cover, and precipitation. ArcGIS and its spatial extensions were used to extract catchment boundaries and stream networks. Lithological descriptions and the geological map were adapted from Tesfamichael's (2009) work on the Geba Basin (Figure 2).

Lineaments, lineament density, and lineament trend analyses were generated using ENVI 4.5, Geomatica 2012, ArcGIS 10, and RockWorks 15. The hillshade DEM (TIFF format) was transformed using Principal Component Analysis (PCA), and lineaments were automatically extracted from the PCA results using PCI Geomatics 2012. Lineament density was mapped using the Line Density tool in ArcGIS 10, while dominant lineament orientations were assessed in RockWorks 15. Drainage and lineament densities were produced using the Line Density function in the Spatial Analyst tool.

Landsat 8 OLI imagery was downloaded from the U.S. Geological Survey Earth Explorer platform to prepare the land use/land cover map through interactive supervised classification in ArcGIS 10. The soil map was compiled from earlier works by Tesfamichael (2009) on the Geba Basin and Berhe et al. (2020) on the Illala–Aynalem sub-basins. Additionally, 16 primary soil samples were collected during the 2016 field campaign and analyzed for textural properties at Mekelle University's Department of Civil Engineering to verify inconsistencies in previous datasets.

Deep-well groundwater data were obtained from the Mekelle Water Supply Service Office, while shallow well and spring data were collected during field surveys conducted between 2016 and 2019.

2.2.2. Multi-criteria decision analysis using AHP

The weighted overlay analysis of the thematic layers and feature classes in this study were made using the concepts of Analytical Hierarchical Process (AHP). The AHP method is used to generate and integrate all thematic layers based on their importance and influences for groundwater prospect. The multi-criteria decision analysis using Analytical Hierarchical Process (AHP) is the most common GIS-based method for demarcating groundwater prospect zones (Arulbalaji et al., 2019). According to Saaty (1988 and 2005) weight criteria decision of the AHP is based on assignment of scales for pair wise comparison of the

thematic layer's matrix. Thematic layers with equal importance for groundwater prospect are assigned 1 but for the extreme importance of the pairs a rate of 9 is given (Saaty, 1988 and 2005). This assignment is applied for both the class of the layers and the thematic layers to identify their ranks and priority for the groundwater prospect. Therefore, the total weight (TW) is determined from the assigned weights and the normalized weight (NW) is average of the matrix values derived from the assigned weight of the thematic layers and feature classes divided by the corresponding total values (Table 1). The thematic layer with a higher normalized weight value shows a higher influence where as a lower value illustrates a less important on the groundwater prospect zones (Magesh et al., 2012). The principal Eigenvalues of the parameters and class are derived from the product of the corresponding total weight and normalized weight. The max values of the thematic layers and classes (largest Eigenvalues) are computed from the summation of the product of total and normalized weights of the parameters in the matrix to check the decision consistency of the pair wise comparison as shown in Equ. 1.

$$\lambda_{max} = \sum_{i=1}^{n} TW_i * NW_i \quad \textbf{..... Equ. 1}$$

Where λ_{max} stands for the largest Eigenvalues, TW_i for the total weight and NW_i for the Normalized weight of the thematic layers and feature classes.

The consistency index was defined as the measure of consistency, deviation or degree of variation of consistency and computed using (Equ. 2) and proposed by Saaty (1988) to use the consistency index by comparing with the appropriate consistency index so-called Random consistency index (RI) (Saaty, 1988). The comparison between the consistency index (CI) and random consistency index (RI) is called consistency ratio (CR) which is computed using Equ. 3. Value of this Consistency Ratio should be smaller or equal to 0.1 to accept judgment of the weight assignments in the matrix (Saaty, 1988).

$$CI = \frac{(\lambda_{max} - n)}{(n-1)} \quad \text{.....Equ. 2}$$

Where CI stands for consistency index, λ_{max} for the largest Eigen values and n is n^{th} number of the thematic layers and feature classes.

$$CR = \frac{CI}{RI} \text{ ..... Equ. 3}$$

Where CR stands for consistency ratio, CI for consistency index and RI for random consistency index.

Table 1. Assigned weights of each thematic layer and the derived total and normalized weights of the thematic layers (CI = 0.081 and CR = 0.057).

TL	GMLF	Geo	LD	SP	DD	SL	LUC	PPT	NW
GMLF	1.00	2.00	3.00	2.00	2.00	2.00	2.00	2.00	0.22
Geo	0.50	1.00	2.00	2.00	3.00	4.00	4.00	5.00	0.21
LD	0.33	0.50	1.00	2.00	4.00	4.00	6.00	6.00	0.20
SP	0.50	0.33	0.50	1.00	2.00	4.00	5.00	5.00	0.15
DD	0.50	0.25	0.33	0.50	1.00	2.00	4.00	4.00	0.09
SL	0.33	0.20	0.25	0.33	0.50	1.00	2.00	2.00	0.06
LUC	0.25	0.17	0.20	0.25	0.33	0.33	1.00	2.00	0.04
PPT	0.20	0.14	0.17	0.20	0.20	0.33	1.00	1.00	0.03
TW	3.62	4.59	7.45	8.28	13.03	17.67	25.00	27.00	1.00

Where TL – Thematic Layers, GMLF – Geomorphology landform, Geo – Geology, LD – Lineament Density, SP – Slope, DD – Drainage Density, SL – Soil, LUC – Land Use/Cover, PPT– Precipitation, TW – Total Weight and NW – Normalized Weight.

2.2.3. Weighted overlay analysis for groundwater prospect zonation

Weighted sum overlay analysis of the thematic layers was made in ArcGIS based on the computation of groundwater prospect index presented in Equ. 4. The derived normalized weights of the thematic layers and feature classes were presented in Table 2. These layers were reclassified based on their importance to groundwater prospect and were exported to tiff files with the cell size of 12.5 meters to generate the groundwater prospect zones using the weighted sum overlay analysis in ArcGIS.

$$GWPI = (GMLF_w * GMLF_{wi}) + (Geo_w * Geo_{wi}) + (LD_w * LD_{wi}) + (SP_w * SP_{wi}) + (DD_w * DD_{wi}) + (SL_w * SL_{wi}) + (LUC_w * LUC_{wi}) + (PPT_w * PPT_{wi}) \quad \text{..... Equ. 4}$$

Where: GWPI refers to groundwater prospect index, GMLF for geomorphology, Geo for geology, LD for lineament density, SP for slope, DD for drainage density, SL for soil texture, LULC for land use land cover, PPT for precipitation and the subscripts of w and wi are for the normalized weights of the themes and normalized weights of the feature class, respectively.

Table 2. Classes of the thematic layers with their normalized weights

Thematic layers (w)	Classes	Wi	Thematic layers (w)	Classes	Wi
GMLF (0.22)	CI=0.091, CR=0.06		Geo (0.21)	CI=0.076, CR=0.05	
	Plains	0.29		Alluvium	0.32
	Valley	0.21		Upper sandstone	0.22
	Open slopes	0.15		Lower sandstone	0.15
	Upper slopes	0.11		Trap basalt	0.11
	Mid slope drainage	0.08		Limestone-Marl	0.08
	Stream	0.06		Marl-Limestone	0.05
	Upper drainage	0.04		Dolerite	0.04
	Local ridges	0.03		Shale-Marl-Limestone	0.03
	Mid slope ridges	0.02		Shale	0.02

	High ridges	0.02			
LD (0.20)	CI=0.013, CR=0.011		SP (0.15)	CI=0.034, CR=0.030	
	Very high (1.04-1.29)	0.42		Flat (0-4.79)	0.40
	High (0.774-1.03)	0.26		Gentle slope (4.8-10.2)	0.29
	Medium (0.516-0.773)	0.18		Medium slope (10.3-17.1)	0.16
	Low (0.259-0.515)	0.09		Steep slope (17.2-26.6)	0.09
	very low (0.0-0.258)	0.05		Very steep (26.7-76.3)	0.05
DD (0.09)	CI=0.015, CR=0.025		SL (0.06)	CI=0.01, CR=0.012	
	Low (0-0.3)	0.54		Sandy clay loam	0.45
	Medium (0.31-0.75)	0.30		Silty loam	0.34
	High (0.76-1.92)	0.16		Silty clay loam	0.14
				Clay Loam	0.07
LUC (0.04)	CI=0.046, CR=0.035		PPT (0.03)	CI=0.013, CR=0.011	
	Water body	0.35		713-822	0.42
	Agricultural land	0.24		634-712	0.26
	Grass land	0.16		563-633	0.18
	Forest land	0.11		503-562	0.09
	Shrub	0.07		434-502	0.05
	Bare land	0.05			
	Residential	0.03			

3. RESULTS AND DISCUSSION

4.1 Thematic layers

Geology

Geology of the study area which is part of the Mekelle outlier is mainly composed of six geological formations namely the alluvial deposit, Mekelle dolerite, Ambaradom sandstone, Agulae shale, Antalo limestone and Adigrat sandstone. It is known that in hydrogeological point of view, areas covered with the alluvial deposits are the main groundwater prospect areas.

The weight assignment of the geology classes in the AHP is therefore based on these concepts of hydraulic properties, degree of fracturing and extent of areal coverage for each geological formation exposed in the study area. Numerical matrix weights for each geology class pairs of the nine geology classes were assigned and tabulated based on their relative importance with respect to groundwater prospect using the numerical rates and reciprocals (Saaty, 1988 and 2005). Consequently, a tabulated pair matrix of the normalized weight of each geology feature class was derived and this derived matrix provides normalized

weights ranging from the lowest in Shale (0.02) to the highest in alluvial deposits (0.31) as presented in Table 2.

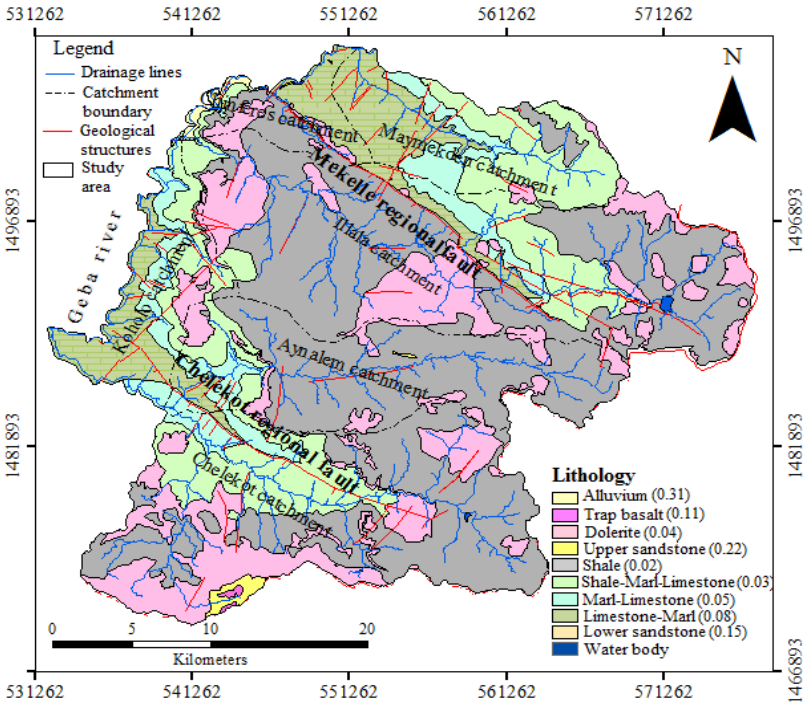


Figure 2. Geological map of the study area (Tesfamichael, 2009).

Geomorphologic Landform

Terrain analyses of different landform classes are made from the digital elevation model based on the topographic position index (TPI) terrain classification in SAGA GIS software (Conrad et al., 2015). According to Weiss (2001) a landform class using TPI is the difference between the elevation value of each cell in a digital elevation model (DEM) and the average elevation of the specified neighborhood around that cell. Negative values (valley) mean the cell is lower than its surroundings while Positive values (ridge) mean it is higher.

The study area in this work is therefore classified into ten classes as: plain, valley, open slope, upper slope, mid slope drainage, streams, upland drainage, local ridge, mid slope ridge, and high ridges. These ten classes were paired to constitute a numerical matrix with respect to their relative importance for groundwater prospect through the numerical rates and reciprocals (Saaty, 1988 and 2005). Accordingly, the derived tabulated pair matrix of the normalized weights for each landform feature class gives normalized weights ranging from the lowest in high ridge (0.01) to the highest in plain landform (0.29) as presented in Table 2 and Figure 3.

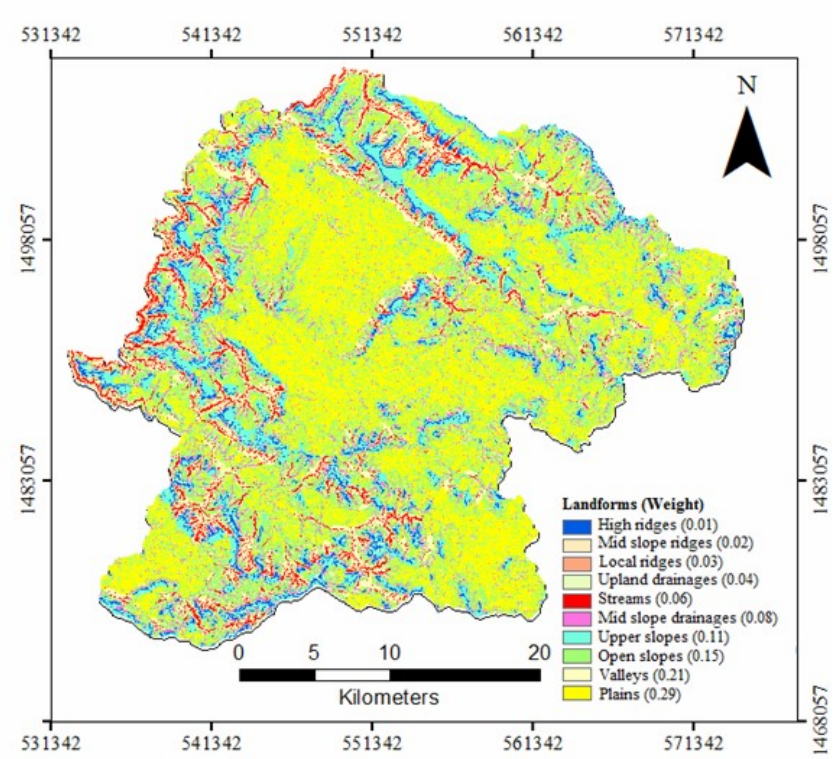


Figure 3. Geomorphologic landforms map.

Lineament and Lineament density

Lineaments are the linear features such as fault, joint, and fractures which serve as a container and conduit for groundwater storage and movement (Reddy et al., 2000; Mukherjee et al., 2012). Accordingly, the groundwater movement and storage in hard rocks are controlled by lineaments and discontinuities because they are considered as subsurface secondary porosity. The intersections of various lineaments are areas where groundwater storage is possible keeping other parameters favorable for groundwater infiltration and storage.

On the other hand, map of the lineament density (the ratio of the total lineament lengths and the unit area expressed as Km per Km^2) is important to reveal the groundwater recharge, flow, and development (Nag and Saha, 2014; Murasingh e al., 2018). The lineaments in the research area are trending NW-SE directions as indicated in the rose diagram (Figure 4). The lineament density is concentrated in the northeastern and southwestern parts of the area and it is sparse in the central part. Therefore, areas with higher lineament density have high groundwater prospect as they are associated with the other parameters like landform and slope. The lineament density of the study area is developed from the lineaments and its values are classified into five based on equal interval classification as: 0 to 0.258 (very low), 0.259 to

0.515 (low), 0.516 to 0.773 (medium), 0.774 to 1.03 (high) and 1.04 to 1.29 km/km^2 (very high). Finally, the highest weight was assigned for the highest lineament density for the groundwater prospect zone mapping as indicated in Table 2 and Figure 4.

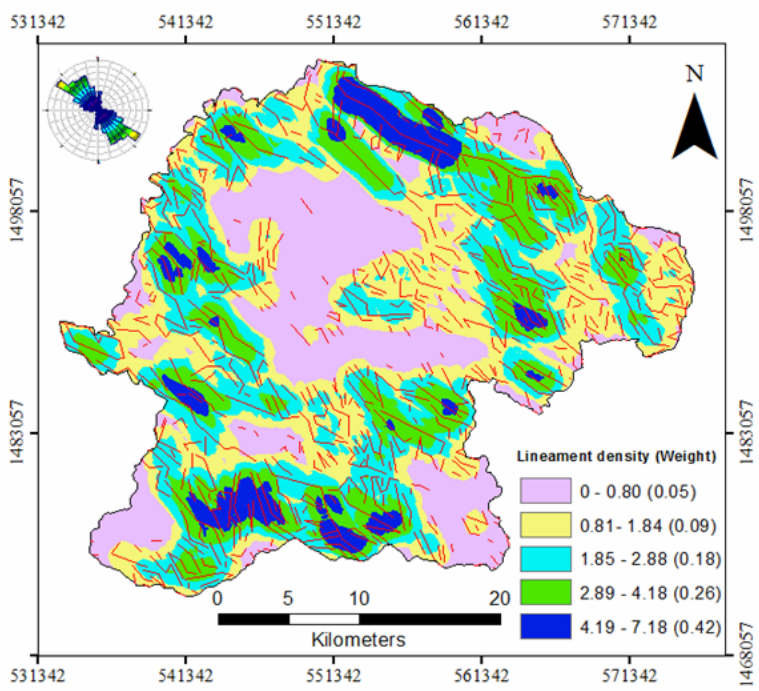


Figure 4. Lineaments, lineament density and rose diagram of the lineaments

Slope

According to Morbidelli et al. (2018) slope is one of the factors controlling the processes of infiltration of surface water into the subsurface. Slope plays an important role to enhance and shrink groundwater prospect of a drainage system as the infiltration rate is increasing with decreasing of the slope angle. The slope thematic layer of the catchments in the study area is directly derived from the topography map using the 'derive slope' module in ArcGIS 10. The slope angle ranges from 0º – 76º and is classified into five slope classes: as 0 to 4.79 degrees (flat plain), 4.8 to 10.2 degrees (gentle slope), 10.3 to 17.1 degrees (intermediate), 17.2 to 26.6 degrees (steep) and 26.7 to 76.3 degrees (highly steep).

The lower slope angle is very important for groundwater percolation whereas the highly steep slope promotes surface runoff. The northwestern and western cliffs and deep gorges with a rugged topography are susceptible to runoff, whereas the eastern high land plateaus and the central plains associated with a

low slope are important for infiltration. Therefore, the highest weight is assigned for low slope (flat plain) and the lowest weight is given for the very steep slopes (Table 2 and Figure 5).

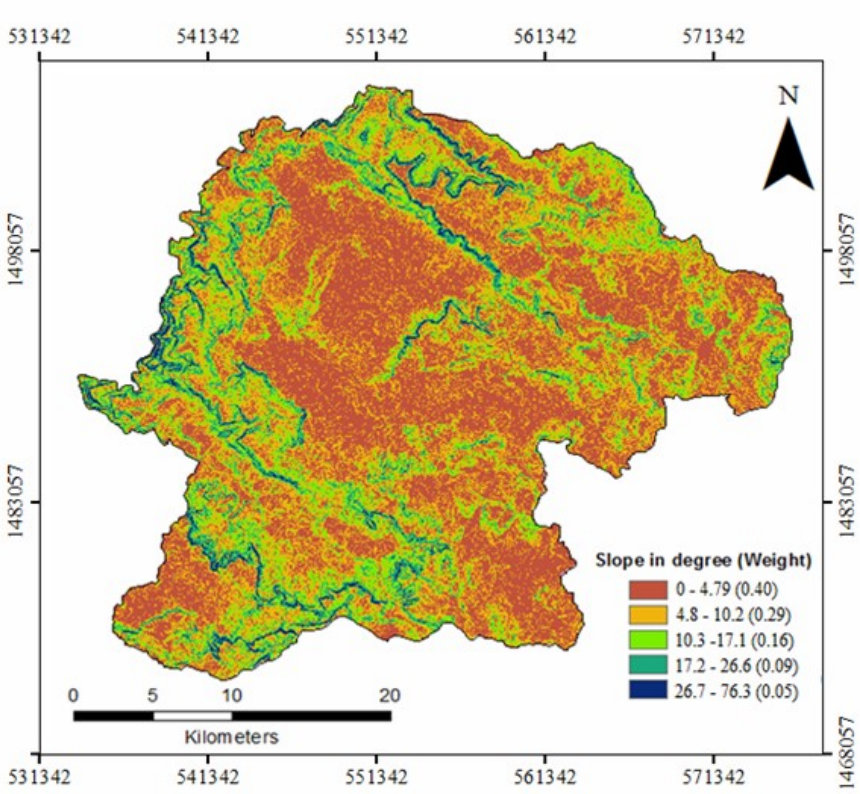


Figure 5. Slope map of Mekelle area

Drainage Pattern and Drainage Density

According to Singhal and Gupta (2010), drainage characteristics of a basin provide an indirect clue to the hydrogeological characteristics of the area and are useful for groundwater resources assessment. The main drainage characteristics are drainage patterns and drainage density. Singhal and Gupta (2010) also state that the drainage density of an area shows the nature of relief, climate, resistance to erosion and permeability of the rock materials. Moreover, the area with high drainage density indicates the high relief, low resistant to erosion, low permeability, high surface runoff, and very low groundwater recharge and the reverse is true for low drainage density area. Drainage density is the ratio of the total channel length of the streams to the total area and is high in areas where more streams confluent (Eq. 5).

$$DD = \sum \frac{L}{A} \quad \text{..... Eq. 5}$$

Where DD is drainage density, L is the total length of the streams, and A is total catchment area.

The study area is drained by four main rivers, namely the Chelekot, Aynalem, Illala and May Mekden that flow from east to the west directions and join the Geba River in the western boundary. These streams are seasonal where the peak discharge is attained during summer. The general river course coincides with the main fault system in the area, which are concentrated along belts running echelon with a west-north-west direction (Beyth and Shachnai, 1970).

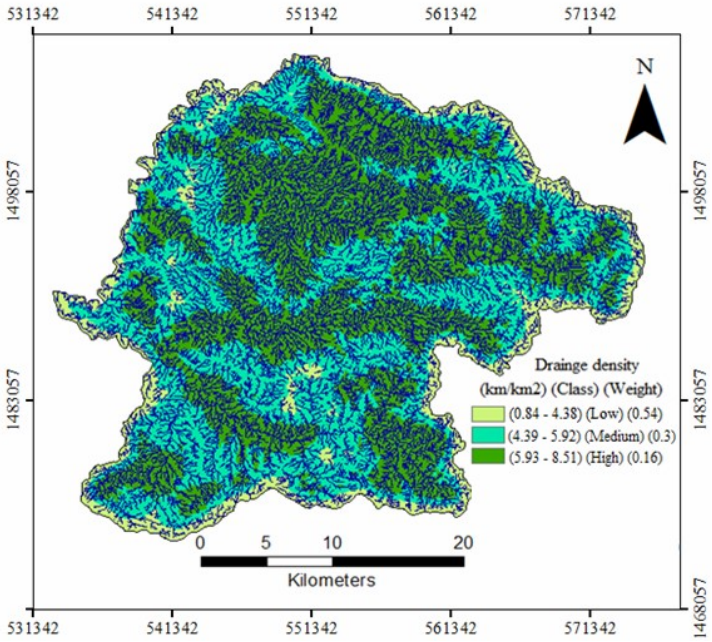


Figure 6. Drainage lines and drainage density map of the study area.

However, many seasonal tributaries feed the main stream both from north and south with substantial amount of runoff water during the rainy season. The drainage density of the study area with total length of stream network (626.82 km) and total area of (1,037.91 km^2) is (0.60 km/km^2) and the streams have a dendritic drainage pattern (Figure 6). Therefore, this drainage density map is divided into three main classes as: 0 to 0.3 for low, 0.31 to 0.75 for medium, and 0.76 to 1.92 for high drainage density. Low weight is given for high drainage density while high weight is given for the low drainage density of the area (Table 2 and Figure 6).

Soil

Evenly distributed primary soil samples from the study area were collected and analyzed using sieve analysis technique (Table 3) to verify some mismatch among the previous works and develop the soil map representing the study area (Figure 7). The developed soil map (Figure 7) shows that the major soil textures of the study area are classified in to four: Sandy clay loam (22.84 %), Silty loam (1.98%), Clay loam

(48.11%) and Silty clay loam (27.03%). Groundwater recharge zones are places where the ground surface allows water infiltration and percolation through the soil (Chowdhury et al., 2010). The rate of water infiltration directly depends on the grain size of the soils.

Table 3. Soil samples analyzed for the physical textural parameters in this study.

S.No	Sample ID	Location			Soil texture
		X	Y	Z	
1	SS-01	558986	1489830	2235	Silty clay loam
2	SS-02	554512	1487321	2194	Silty clay loam
3	SS-03	556098	1491775	2150	Clay loam
4	SS-04	556671	1494741	1748	Clay
5	SS-05	554362	1487278	2189	Clay
6	SS-06	555227	1488599	2236	Clay loam
7	SS-07	555642	1487498	2205	Clay
8	SS-08	556376	1487482	2220	Sandy loam
9	SS-09	557174	1487913	2225	Silty clay loam
10	SS-10	558242	1485839	2314	Silty loam
11	SS-11	547336	1505890	1800	Sandy clay loam
12	SS-12	538616	1497897	1702	Sandy clay loam
13	SS-13	545520	1480214	1896	Silty clay loam
14	SS-14	556989	1478111	2190	Silty clay loam
15	SS-15	545883	1476459	1928	Sandy clay loam
16	SS-16	540312	1473674	2208	Silt clay loam

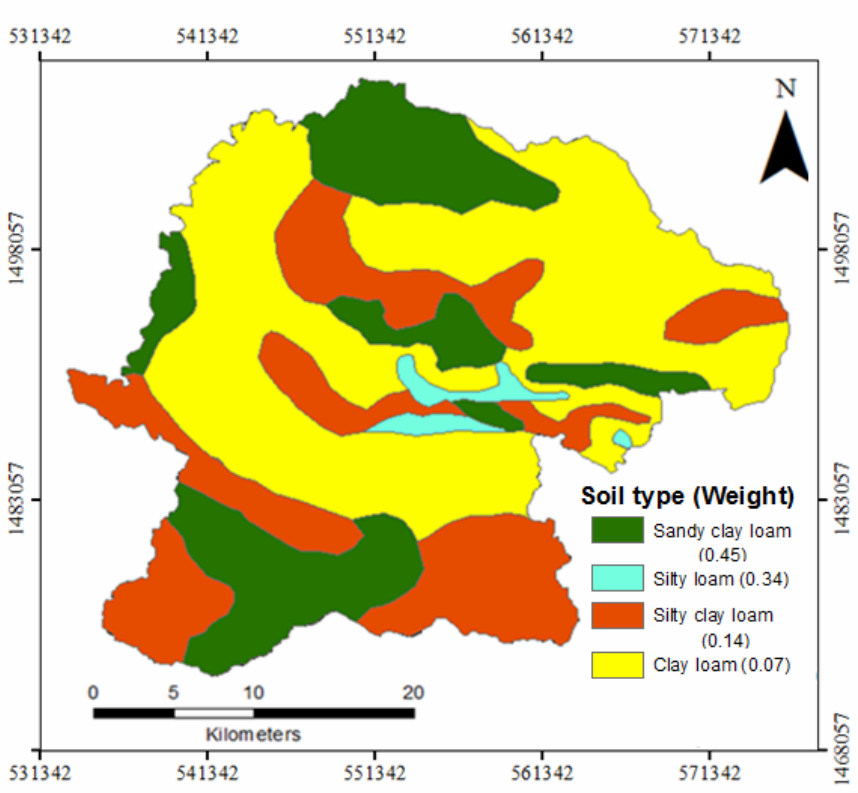


Figure 7. Soil map of the study area.

Soil textures are a valuable thematic layer for groundwater prospect and recharge assessment. Soil texture, the percentage of sand, silt, and clay, is an inherent factor affecting infiltration, percolation, and recharge. Water moves more quickly through large pores of sandy soil than through clayey soil. The sandy soils have a high infiltration rate than clayey soils. Consequently, weights are assigned for the different soil classes in the study area with the highest values for sand clay loam (0.45) and lowest values for clay loam (0.07) as presented (Table 2 and Figure 7).

Land use/cover (LULC)

Accurate and reliable information about the present and future LULC will support in the management of water resources (Murmu et al., 2019; Singh et al., 2019). Understanding the effect of LULC on groundwater recharge and surface runoff is very important for sustainable water resource management (Owuor et al., 2016). The satellite digital images of (row number 51) and (path numbers 168 and 169) captured on February 14 to 22, 2018. The two images for each path number have been mosaicked and masked to smaller size, fitting the study area boundary using raster management and extraction tools in ArcGIS 10. Training samples were assigned using different (RGB) band combinations for Landsat 8 and

the interactive supervised image classification in ArcGIS 10 was also used to develop the LULC map of the study area.

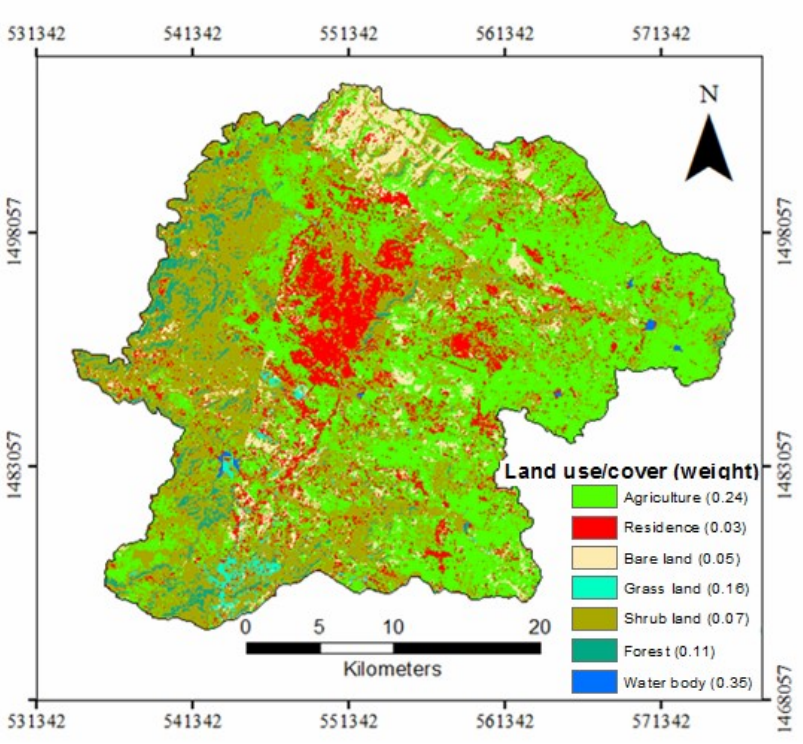


Figure 8. Land use/ land cover map of the study area.

The developed LULC map consists of seven LULC classes namely: cultivated agricultural land with scattered trees (30.75 %), shrub land (38.55%), bare land (7.57%), grass land (1.47%), water body (4.85%), settlement of rural community and urban areas (15.09 %) and forest (1.72%) (Figure 8). The land LULC map was verified using 458 ground truth LULC points collected with Garmin GPS (Table 4). These ground observation points were randomly identified up on several field visits of the inventory of the springs, shallow and deep wells during the period 2014 to 2020. Moreover, it is known that precipitation has a tendency to infiltrate in the forest, vegetated and agricultural lands and to flow as surface runoff on the bare land and residential area. The highest weight is therefore assigned to the water body (0.35) and cultivated land (0.24) and the lowest to bare land (0.05) and residential (0.03) (Table 2 and Figure 8).

Table 4. Results of the ground truth verification for the land-use/cover map

Land-use class (observation)	Number of GPS points with ground truth	**land-use class(map)**							
		Bare land	Grassland	Shrub land	Agriculture	Forest	Residence	Water body	Correspondence (%)

Bare land	49	46	0	1	2	0	0	0	**93.88**
Grassland	25	0	19	2	4	0	0	0	**76.00**
Shrub land	101	2	2	84	8	5	0	0	**83.17**
Agriculture	155	3	2	2	143	0	4	1	**92.26**
Forest	19	3	0	2	0	14	0	0	**73.68**
Residence	65	5	7	0	2	0	51	0	**78.46**
Water body	12	0	2	0	0	0	0	10	**83.33**
					total 458		**mean correspondence (%)**		**82.97**

Precipitation

The mean annual precipitation of the study area varies from 391 to 646 mm/year and its spatial distribution is produced using the spline interpolation method in ArcGIS 10 software.

The precipitation data was taken from the Mekelle observational station (Mekelle OBS), Mekelle Airport, Illala Research Center (Illala RC), Hagere Selam, Agulae, Aragure, Sheket, Adigudom and Dengolat metrological stations. The precipitation distribution is high in the high land plateaus in the northeastern part and low in the southwestern low lands of the study area. According to Agarwal et al. (2013), precipitation is the main source of groundwater recharge. The precipitation distribution in the study area was classified into five as: 391 to 443, 444 to 497, 498 to 544, 545 to 584 and 585 to 646 mm/year (Figure 9). Highest weight was assigned for the high precipitation because of its high importance for groundwater prospect and vice versa (Figure 9).

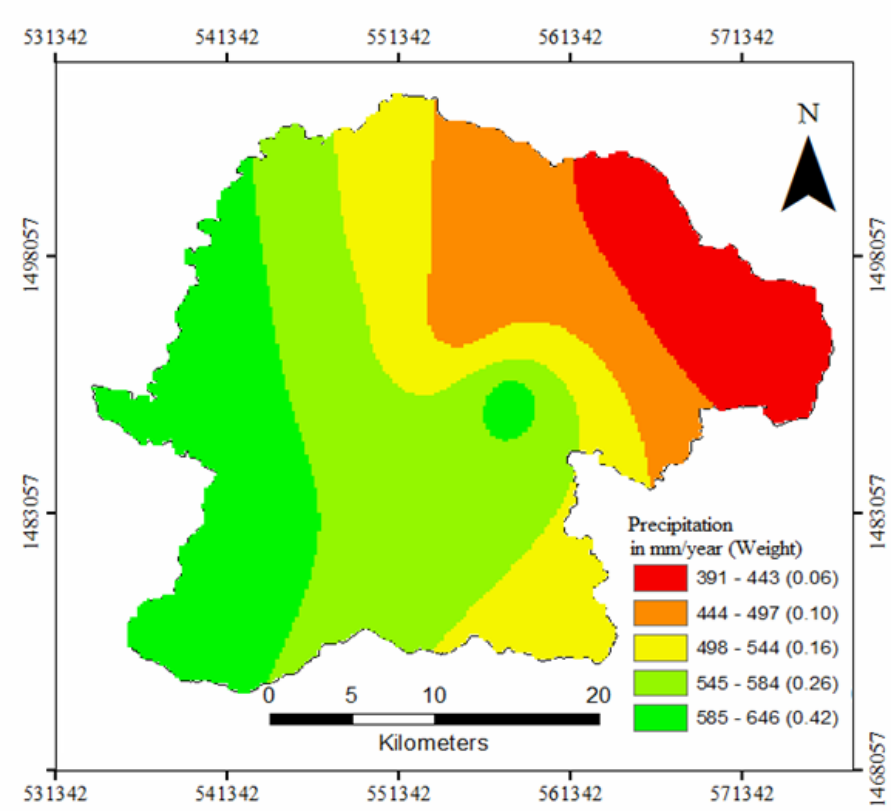


Figure 9. Spatial distribution of precipitation

4.2 Groundwater prospect zones

Results of the weighted sum overlay analysis using the thematic layers indicated four discrete groundwater prospect zones as: very good, good, moderate, and poor groundwater prospect areas (Figure 10). The very good groundwater prospect covers about 34.49% of the total area and the areal percentage of good, moderate, and poor are 23.41%, 24.28%, and 17.82%, respectively (Table 4). The very good and good groundwater prospect zones are found in the alluvial deposits and areas with swarm of lineaments. The moderate and poor groundwater zones are distributed throughout the study area and mainly concentrated in areas with high drainage density.

4.3. Validation

The resulting groundwater prospect map of the study area is validated using yields of the existing 100 groundwater points (springs (29), deep (42) and shallow wells (29)). For this purpose, yields of the groundwater points in the area were classified into four groups as: <1, 1.01 to 16.86, 16.87 to 25.23 and 25.24 to 33.06 L/s (Table 4). These descriptive yield ranges of the water points were classified based on

their intended water use on the water supply of Mekelle city, which further used to validate the groundwater prospect zones in the study area.

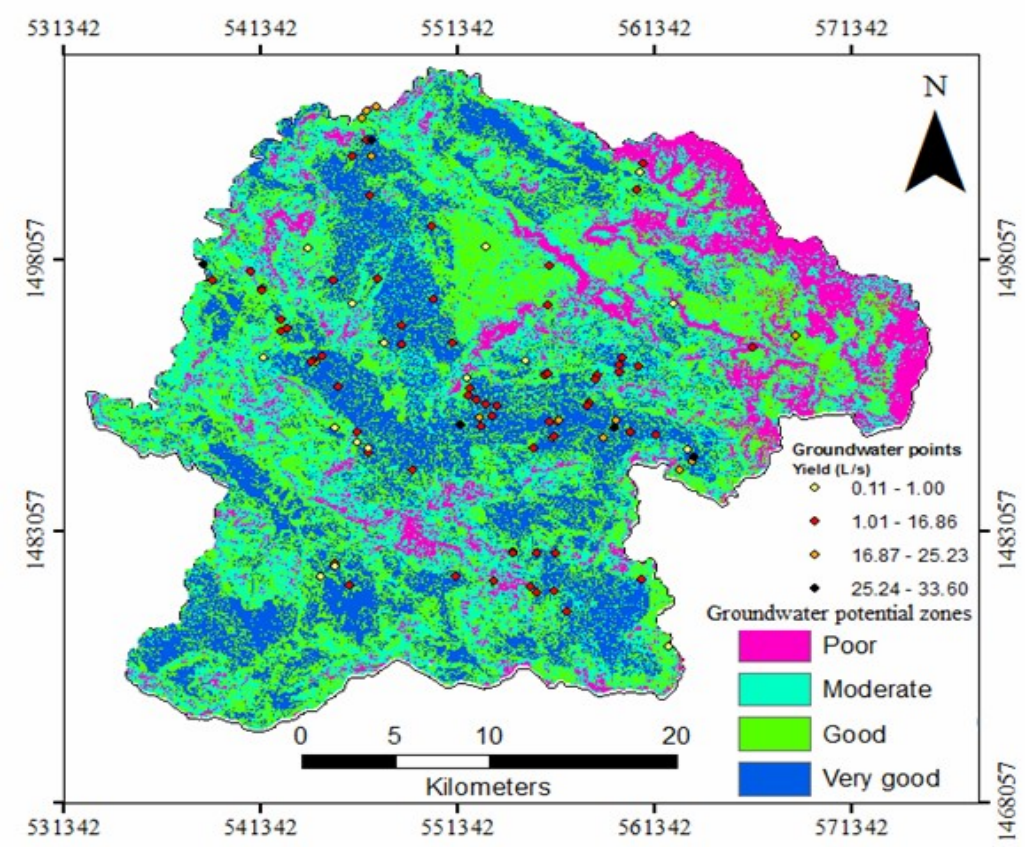


Figure 10. Groundwater prospect zones and validation water points (springs, shallow and deep wells)

Generally, about 83% of the groundwater prospect zones are best fit to the yields of the water points and about 11% are fairly fit as indicated in Table 4. However, there are about 6% exceptions with very high yield located on the poor groundwater prospect zones and vice versa.

Most of these exceptional groundwater points indicated in Table 4 are located in the weak zones of both the regional and synthetic faults and hence taping nearby prospect zones. This phenomenon possibly indicates that the dolerite dikes and fractures are acting as barriers and conduits within localities as the study area is affected with both the dikes and intensive fractures. As a result, some springs and shallow wells with low yield (<1L/s) are distributed among the good and very good prospect zones and some water points with moderate (1.01 to 16.86 L/s) to high (16.87 to 25.23) yield are found in the poor prospect zone.

Table 4 Validation of the resulting groundwater prospect zones. (NA in the table represents no data)

Groundwater prospect zones	Area in Km^2 (Area in %)	Type of water points with their yield classes				Total no. of water points
		Yield classes (L/s)	Springs	Shallow wells	Deep wells	(Best fit, %)(Fair, %)(Exception, %)
Very good	358 (34.49)	< 1.00	SP-09, SP-15, SP-16, SP-23	SW-17	NA	56 (51, 91.07)(0, 0.00)
		1.01 – 16.86	SP-07, SP-10, S SP-14, SP-17, SP-24, SP-27	SW-04,SW-05,SW-06,SW-07,SW-08,SW-10, SW-11,SW-13,SW-14, SW-16,SW-18,SW-23, SW-24,SW-25,SW-27, SW-28	DW-02,DW-06,DW-07,DW-10, DW-12,DW-14,DW-15,DW-18, DW-20,DW-21,DW-22,DW-23 DW-24,DW-29,DW-31DW-35, DW-37,DW-38	(5, 8.93)
		16.87 – 25.23	NA	NA	DW-13,DW-11,DW-26,DW-39, DW-40, DW-42	
		25.24 – 33.60	SP-19, SP-28	NA	DW-01, DW-19, DW-41	
Good	243 (23.41)	< 1.00	SP-04,SP-11, SP-22, SP-26	SW-19	NA	22 (17, 77.27)(5, 22.73)
		1.01 – 16.86	SP-03,SP-18, SP-25, SP-29	SW-02,SW-09,SW-15, SW-26	DW-03,DW-08,DW-16,DW-33, DW-34, DW-36	(0, 0.00)
		16.87 – 25.23	NA	SW-29	DW-05, DW-17	
Moderate	252 (24.28)	< 1.00	SP-02	SW-12, SW-20, SW-21	NA	16 (13, 81.25)(3, 18.75)
		1.01 – 16.86	SP-05,SP-06, SP-08,SP-20, SP-21	SW-03	DW-25, DW-28, DW-30	(0, 0.00)
		16,87 – 25.23	NA	NA	DW-04, DW-09, DW-27	
Poor	185 (17.82)	1.01 – 16.86	SP-01,SP-12, SP-13	SW-01, SW-22	NA	6 (2, 33.33)(3, 50.00)
		16.87 – 25.23	NA	NA	DW-32	(1, 16.67)
Validation results						100 (83, 83.00%)(11, 11.00% (6, 6.00%)

4. CONCLUSION

Application of the AHP technique is successful in generating reliable results of groundwater prospect zones. The success of the AHP method is confirmed with the verification result of the yields in 100 existing groundwater points with about 94% fit (85% best fit and 9% fairly fit). The groundwater prospect zones are best fit to the yields of the water points with some exceptions having very high yield located on the poor groundwater prospect zones and vice versa. In general results of the AHP using weighted sum overlay analysis of the thematic layers is useful to provide reasonable groundwater prospect zone classes. Hence, this study can therefore be used to the management and planning of new groundwater-based projects in the study area.

ACKNOWLEDGEMENTS

We are thankful to the MU-IUC VLIR-UOS project office members at Mekelle University for their logistical support. The authors also thank the Ethiopian National Meteorology Agency for providing meteorology data. Furthermore, this work was kindly supported by Mekelle University Contract Research and Publication Team (CRPT) providing fund for part of the field work in this study.

REFERENCES

Abdelwassie, H. (2000). Hydrogeology of the Aynalem Wellfield, Tigray, Northern Ethiopia. Unpublished Msc thesis, Addis Ababa University.

Agarwal, E., Agarwal, R., Garg, R.D. and Garg, P.K. (2013). Delineation of groundwater potential zone: An AHP/ANP approach. *Journal of earth system science*, 122, 887-898.

Al-Shabeeb, A.A.R., Al-Adamat, R., Al-Amoush, H. and AlAyyash, S. (2018). Delineating groundwater potential zones within the Azraq Basin of Central Jordan using multi-criteria GIS analysis. *Groundwater for Sustainable Development*, 7, 82-90.

Arulbalaji, P., Padmalal, D. and Sreelash, K., (2019). GIS and AHP techniques based delineation of groundwater potential zones: a case study from southern Western Ghats, India. *Scientific reports*, 9(1), 2082.

Beyth, M. and Shachnai, E. (1970). Hydrogeology of Mekelle area. Geological Survey of Ethiopia.

Chowdhury, A., Jha, M.K. and Chowdary, V.M. (2010). Delineation of groundwater recharge zones and identification of artificial recharge sites in West Medinipur district, West Bengal, using RS, GIS and MCDM techniques. *Environmental Earth Sciences*, 59, 1209-1222.

Conrad, O., Bechtel, B., Bock, M., Dietrich, H., Fischer, E., Gerlitz, L., Wehberg, J., Wichmann, V. and Böhner, J. (2015). System for automated geoscientific analyses (SAGA) v. 2.1. 4. *Geoscientific Model Development*, 8(7), 1991-2007.

DAAC, A. (2015). ALOS PALSAR_Radiometric_Terrain_Corrected_low_res; Includes Material© JAXA/METI 2007. Accessed through ASF DAAC. *Available online*: https://doi. org/10.5067/JBYK3J6HFSVF (accessed on 15 December 2020).

Daniel, G. (1977). Aspects of climate and water budget in Ethiopia. Addis Ababa University Press. 71 pp.

Fetter, C.W., 1994. *Applied Hydrology*; Robert A. McConnin.

Gebru, H., Gebreyohannes, T. and Hagos, E. (2020). Identification of groundwater potential zones using analytical hierarchy process (AHP) and GIS-remote sensing integration, the Case of Golina River

Basin, Northern Ethiopia. *International Journal of Advanced Remote Sensing and GIS*, 9(1) - 3289.
Girmay, E.H. (2015). Litho–Structural Controls on the Groundwater Flow System and Hydrogeochemical Setup of the Mekelle Outlier and Surrounding Areas, Northern Ethiopia (Doctoral dissertation, Addis Ababa University).
Gnanachandrasamy, G., Zhou, Y., Bagyaraj, M., Venkatramanan, S., Ramkumar, T. and Wang, S. (2018). Remote sensing and GIS based groundwater potential zone mapping in Ariyalur District, Tamil Nadu. *Journal of the Geological Society of India*, 92, 484-490.
Griffiths, J.F. (1972). Climates of Africa. In "World Survey of Climatology" (HE Landsberg, Ed.).
Ishizaka, A. and Labib, A. (2011). Review of the main developments in the analytic hierarchy process. *Expert systems with applications*, 38(11),14336-14345.
Kebede, S. and Travi, Y. (2012). Origin of the δ18O and δ2H composition of meteoric waters in Ethiopia. *Quaternary International*, 257, 4-12.
Magesh, N.S., Chandrasekar, N. and Soundranayagam, J.P. (2012). Delineation of groundwater potential zones in Theni district, Tamil Nadu, using remote sensing, GIS and MIF techniques. *Geoscience frontiers*, 3(2), 189-196.
Morbidelli, R., Saltalippi, C., Flammini, A. and Govindaraju, R.S. (2018). Role of slope on infiltration: A review. *Journal of hydrology*, 557, pp.878-886.
Mukherjee, P., Singh, C.K. and Mukherjee, S. (2012). Delineation of groundwater potential zones in arid region of India—a remote sensing and GIS approach. *Water resources management*, 26, 2643-2672.
Murasingh, S., Jha, R. and Adamala, S. (2018). Geospatial technique for delineation of groundwater potential zones in mine and dense forest area using weighted index overlay technique. *Groundwater for sustainable development*, 7, 387-399.
Murmu, P., Kumar, M., Lal, D., Sonker, I. and Singh, S.K. (2019). Delineation of groundwater potential zones using geospatial techniques and analytical hierarchy process in Dumka district, Jharkhand, India. *Groundwater for Sustainable Development*, 9, 100239.
Nag, S.K. and Saha, S. (2014). Integration of GIS and remote sensing in groundwater investigations: a case study in Gangajalghati Block, Bankura District, West Bengal, India. *Arabian Journal for Science and Engineering*, 39, 5543-5553.
Nsiah, E., Appiah-Adjei, E.K. and Adjei, K.A. (2018). Hydrogeological delineation of groundwater potential zones in the Nabogo basin, Ghana. *Journal of African Earth Sciences*, 143, 1-9.
Owuor, S.O., Butterbach-Bahl, K., Guzha, A.C., Rufino, M.C., Pelster, D.E., Díaz-Pinés, E. and Breuer, L. (2016). Groundwater recharge rates and surface runoff response to land use and land cover changes in semi-arid environments. *Ecological Processes*, 5(1), 1-21.
Patra, S., Mishra, P. and Mahapatra, S.C. (2018). Delineation of groundwater potential zone for sustainable development: A case study from Ganga Alluvial Plain covering Hooghly district of India using remote sensing, geographic information system and analytic hierarchy process. *Journal of Cleaner Production*, 172, 2485-2502.
Pinto, D., Shrestha, S., Babel, M.S. and Ninsawat, S. (2017). Delineation of groundwater potential zones in the Comoro watershed, Timor Leste using GIS, remote sensing and analytic hierarchy process (AHP) technique. *Applied Water Science*, 7, 503-519.
Reddy, G.O., Mouli, K.C., Srivastav, S.K., Srinivas, C.V. and Maji, A.K. (2000). Evaluation of ground water potential zones using remote sensing data-A case study of Gaimukh watershed, Bhandara District, Maharashtra. *Journal of the Indian Society of Remote Sensing*, 28, 19-32.
Saaty, T.L. (1988). What is the analytic hierarchy process? Springer Berlin Heidelberg, 109-121.
Saaty, T.L. (2005). Theory and applications of the analytic network process: decision making with benefits, opportunities, costs, and risks. RWS publications.
Sar, N., Khan, A., Chatterjee, S. and Das, A. (2015). Hydrologic delineation of ground water potential zones using geospatial technique for Keleghai river basin, India. *Modeling Earth Systems and*

Environment, 1, 1-15.
Sener, E., Davraz, A. and Ozcelik, M. (2005). An integration of GIS and remote sensing in groundwater investigations: a case study in Burdur, Turkey. *Hydrogeology Journal*, 13, 826-834.
Singh, S.K., Zeddies, M., Shankar, U. and Griffiths, G.A. (2019). Potential groundwater recharge zones within New Zealand. *Geoscience Frontiers*, 10(3),1065-1072.
Singhal, B.B., S and Gupta, RP (2010). Applied hydrogeology of fractured rocks.
Siva, G., Nasir, N. and Selvakumar, R. (2017). Delineation of groundwater potential zone in Sengipatti for Thanjavur district using analytical hierarchy process. In IOP conference series: *Earth and environmental science* (Vol. 80, No. 1, 012063). IOP Publishing.
Telford, R.J. (1998). The palaeoenvironmental record of Holocene environmental change in the Ethiopian Rift Valley. Unpublished Ph. D. Thesis, University of Wales.
Tesfamichael, G. (2009). Regional groundwater flow modelling of the Geba basin (Doctoral dissertation, PhD thesis, Free University of Brussels, Belgium).
Thapa, R., Gupta, S., Guin, S. and Kaur, H. (2017). Assessment of groundwater potential zones using multi-influencing factor (MIF) and GIS: a case study from Birbhum district, West Bengal. *Applied Water Science*, 7, 4117-4131.
Weiss, A. (2001). Topographic position and landforms analysis. In Poster presentation, ESRI user conference, San Diego, CA (Vol. 200).
WWDSE. (2007). Evaluation of Aynalem well field and selection of additional prospective boreholes for Mekelle Town Water supply source. Study report, vol. II.
Yeh, H.F., Cheng, Y.S., Lin, H.I. and Lee, C.H. (2016). Mapping groundwater recharge potential zone using a GIS approach in Hualian River, Taiwan. *Sustainable Environment Research*, 26(1), 33-43.

Publisher's Note

Daagu International Journal of Basic and Applied Research remains neutral with regard to jurisdictional claims in published maps and institutional affiliations.